Determination Of CFD Input Parameters For A MWF Spray

Peggy Geier, Hoisan Kim, Ming-Chia Lai, Xingbin Xie
peggygeier@aol.com

Wayne State University, Detroit, MI 48202 USA

Abstract

The purpose of this work was to collect information to be used to determine CFD input parameters when modeling the dispersion of a spray produced from milling with flood cooling. These parameters are the drop size distribution, the data rates, and the velocity vectors of the drops in the spray. Eleven different test conditions were studied involving variations on the coolant flow rate, the cutter angular speed, the type of coolant, and the cutter surface topography. Little difference in the drop size distributions occurred due to variations on the coolant flow rate and the cutter angular speed. Utilizing a coolant with a mist suppressant resulted in a shift forward in the drop size distribution to higher drop diameters. Utilizing a cutter with a smooth surface topography resulted in a shift backward in the drop size distribution to lower drop diameters. The data rates decreased with increasing flow rate and increased with increasing cutter angular speed. The data rates decreased when utilizing the coolant with a mist suppressant and when utilizing the cutter with the smooth surface topography. Both the velocity vector magnitudes and angles decreased with increasing flow rate. Both the velocity vector magnitudes and angles increased with increasing cutter angular speed. The velocity vector magnitude increased when utilizing the coolant with a mist suppressant at a high flow rate but not at a low flow rate. The velocity vector angle decreased when utilizing the coolant with a mist suppressant. Both the velocity vector magnitude and angle decreased when utilizing the cutter with a smooth surface topography.

1. Scope

Metal Working Fluids (MWFs) are the fluids used in manufacturing to flush away the metal chips from machining and to remove heat produced at the tool-part interface. When MWFs are applied to spinning tools the fluid is atomized to a large extent. The very small drops, 10 microns and less, have been determined to be a health hazard by the Occupational Safety and Health Administration (OSHA) Advisory Committee, and a personal exposure mist concentration limit of .5 mg/m^3 is recommended. Mechanical Engineers need to design precise and efficient close capture exhaust systems to meet this indoor air quality recommendation. Design of the exhaust systems entails determining the exhaust hood size, the exhaust hood location, the exhaust rate, and the filter requirements. To design precise and efficient systems software that models indoor contaminant dispersion is required, such as Computational Fluid Dynamics (CFD) software. To perform the dispersion calculations, certain information is needed on the spray introduced into the computational domain of the model as input into the CFD software, specifically the drop size distribution of the spray dispersing, the drop velocity vectors, and the drop mass generation rates.

As discussed in a previous paper [1], characterization of MWF mist produced during wet horizontal facemilling for 7 different test conditions was accomplished utilizing 4 optical techniques. Three of these methods were imaging methods and included recording the trajectory of the sprays produced with a high speed camera system, taking high resolution still images of the sprays, and taking high resolution images of the large drops and ligaments of the spray using a high energy pulsed light source and a magnifying lens. The fourth method was a non-imaging method, utilizing a Phase Doppler Particle Analyzer (PDPA) [2] to measure drop sizes, velocities and rates. The three imaging methods substantiated the results of the PDPA measurements, not only indicating where PDPA data should best be taken, but also predicting the variations in density, as perpetrated in the PDPA data rates. The 7 test conditions, herein referred to as base cases, involved variations on coolant flow rate and on cutter peripheral velocity. This paper will discuss in greater detail the PDPA work done, with emphasis on the experimental results pertaining to the determination of CFD source term input information. Additionally, four other test conditions will be described and the corresponding PDPA data results will be discussed. Two of the additional test conditions involved using a mist suppressant at two base case conditions, while the other two involved using a different milling cutter edge topography at the same base case conditions.

To avoid convolution thus misinterpretation of experimental results, metal cutting was not performed during the testing. Also note that the mass generation rates of the drops were not measured as part of this study.

2. Experimental Setup And Data Collection Procedure

Essentially zero pressure coolant was impinged upon the 25.4 cm diameter milling cutter in the flood cooling mode used in wet machining. A 1.25 cm diameter nozzle impinged the fluid onto the cutter edge in a plane perpendicular to the axis of rotation of the cutter, as shown in the photograph in Figure 1. The cutter edge was 3 cm wide. PDPA data was taken in a single plane where the data rates were the highest, in the center plane of the impinging fluid. By scanning the spray with the PDPA, this was determined to be the highest data rate plane. The PDPA setup was as illustrated in Figures 2 and 3, with the high data rate plane denoted in Figure 3.

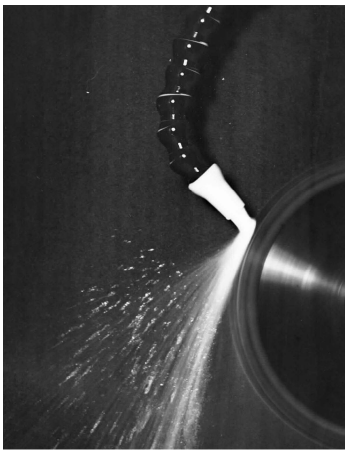

Figure 1. Cutter and nozzle; .126 Lps, 10.1Rps.

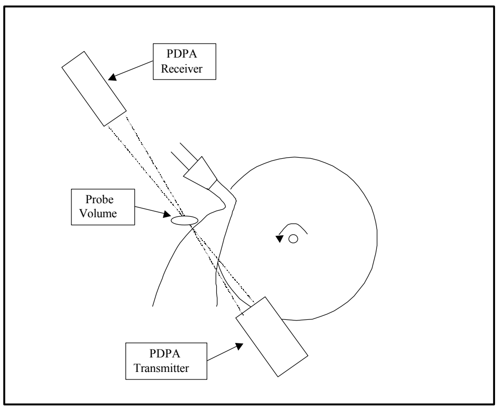

Figure 2. PDPA orientation with respect to MWF spray.

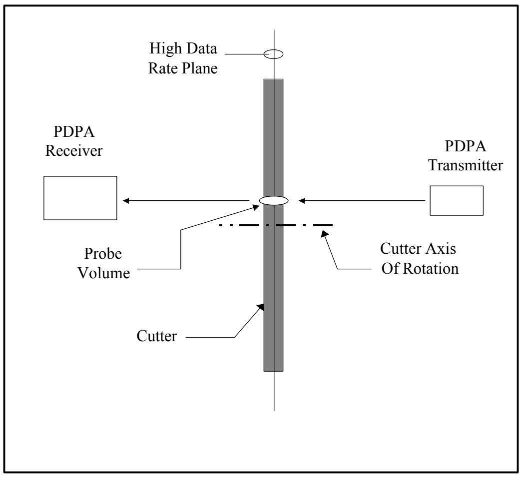

Figure 3. PDPA/MWF spray orientation; front view of cutter peripheral.

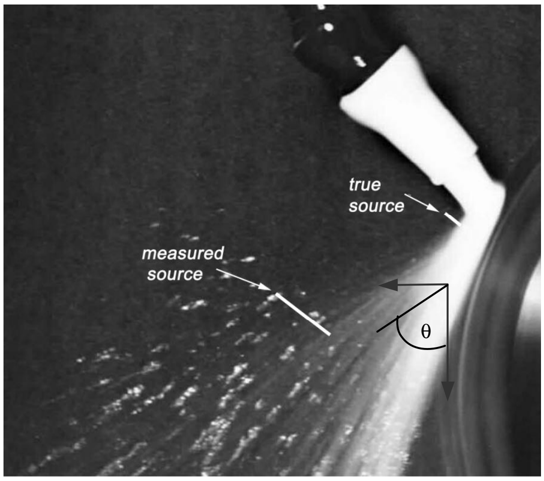

Figure 4. True source versus measured source locations.

Data was taken at numerous points in the region denoted 'measured source' in Figure 4. Only source information is required as CFD input; the CFD algorithms calculate the trajectories and histories of the dispersed phase within the geometrical model thereafter. 'True source' information would be at the location of fluid breakup as denoted in Figure 4. However, at the true source location in the MWF spray, the spray is very dense consisting not only of drops but fluid ligaments. The PDPA cannot size drops when fluid ligaments are dominating the PDPA probe volume, thus the data was taken lower and more to the left where the ligament density was low and the small drop density high. Testing was performed at 11 different test conditions as labeled and described in Table 1. Seven of the test conditions, labeled TC1 through TC7, are the base cases involved variations on the flow rate and on the cutter angular speed. Two of the test conditions, TC8 and TC9, were variations on base cases TC2 and TC7, and utilized a coolant with a polyethylene oxide (PEO) mist suppressant additive [3]. Two of the test conditions, TC10 and TC11, also variations on base cases TC2 and TC7, involved wrapping a smooth aluminum band around the cutter peripheral shown in Figure 3.

3. Experimental Results

3.1. Overall Spray Characteristics

Three characteristic regions were found to exist in all the sprays. Higher up and closer to the cutter edge, essentially closer to the true source, the highest data rate region was found. Here the average number based diameter of the drop size distribution, D10, was relatively small. Because it is the region where most of the drops emanate from, it will henceforth be called the source data region. Below this region and to the left of this region the data rates were lower and the D10s were larger. As the flow rate increased all three of these regions moved farther out from the cutter edge. Relative to the base comparative case, the source data region for the case involving the PEO Additive at the high flow rate (TC9) was found much closer to the cutter edge. This was because of the sheer nature of the MWF with the PEO Additive. The PEO Additive is characterized by a high elongational viscosity resulting in larger drops formed at breakup. The soluble MWF with the PEO Additive is also characterized by a

Table 1. Summary of spray characteristics

TC #	Flow Rate (L/s)	Angular Speed (Rev/s)	Description	Data Rate (counts/s)	Velocity (m/s)	*Spray Angle θ (degrees)	D10 (μm)	Peak Diameter (μm)
TC1	.126	10.1	Base case	6.17	2.21	47.2	67.4	28
TC2	.126	16.7	Base case	25.7	3.28	51.8	64.3	31
TC3	.221	5.92	Base case	1.03	1.30	39.0	67.8	24
TC4	.221	10.1	Base case	5.11	1.67	34.9	66.9	28
TC5	.221	16.7	Base case	17.4	2.97	46.8	61.4	30
TC6	.315	10.1	Base case	5.11	2.09	33.7	68.3	29
TC7	.315	16.7	Base case	17.6	3.07	42.6	63.6	31
TC8	.126	16.7	With PEO	18.9	2.43	41.3	78.1	54
TC9	.315	16.7	With PEO	14.0	3.85	33.4	72.6	51
TC10	.126	16.7	Smooth topography	7.44	1.36	21.9	57.9	25
TC11	.315	16.7	Smooth topography	5.84	1.73	34.2	52.0	28

*Spray angle as shown in Figure 4.

higher molecular weight than soluble MWF without the PEO Additive. Thus the fluid formed much larger drops that fell closer to the cutter edge due to the influence of gravity.

Regarding the Smooth Topography Testing, the spray had four notable differences in character relative to that formed from the cutter topography with the inserts. The source data regions were located at a lower location, the sprays were more disperse, the sprays were more uniform, and the areas over which relatively high data rates existed were wider relative to the comparative base cases. All four of these phenomena were due to the absence of funneling of the fluid with the smooth band. This funneling of the fluid due to the inserts can be seen in Figure 1.

The combined and averaged data rate, drop size distribution and velocity vector was calculated for the source data region. These values are summarized in Table 1 for each test condition. The velocities listed in Table 1 are the average for the drop size range of .75 and 30 μm. In a MWF mixture of 5% concentrate/95% water, drops 30 μm and less are able to evaporate down to a maximum size of 10 μm. This is based on the assumptions that the spray has a uniform amount of concentrate in each drop at breakup, that the concentrate is nonvolatile, and that the concentrate molecules coalesce in the drops as the water evaporates.

3.2 Drop Size Distributions In The Source Data Region

Shown in Figures 5a and 5b are comparisons of the data for the base cases. Figure 5a shows the change in the distributions with increasing cutter angular speed. The greatest apparent difference is at the lowest angular speed; the curve has a much narrower peak relative to the comparative peaks at the two higher angular speeds. There is also a pronounced plateau region between 90 and 125 μm. Comparison of the curves in Figure 5a indicates that the drop size distributions appear to become flatter as the angular speeds increase. This may be due to more thin ligaments (versus fluid sheets) forming as the cutter angular speed increases, dispersing into a spectrum of drops, as well as a higher rate of coalescence of smaller drops. Figures 5b indicate that little difference occurs in the drop size distributions as the flow rate increases at 16.7 Rev/s. There is a plateau region at these 2 angular speeds between approximately 95 and 130 μm, and it appears to almost be a small second peak at .126 L/s. The same behavior was observed at 10.1 L/s over the range of flow rates. A quantitative comparison to investigate if there were statistical differences in the data was also done by

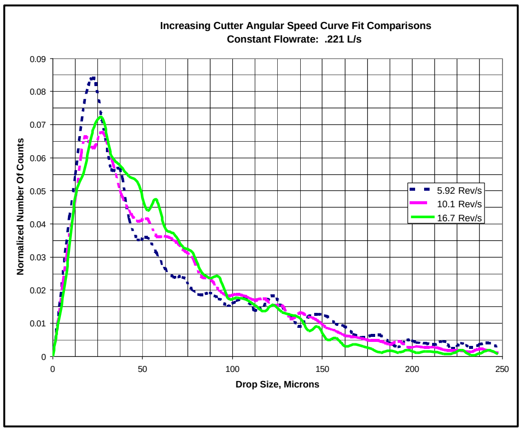

Figure 5a. Drop size distributions for base cases; increasing angular speed.

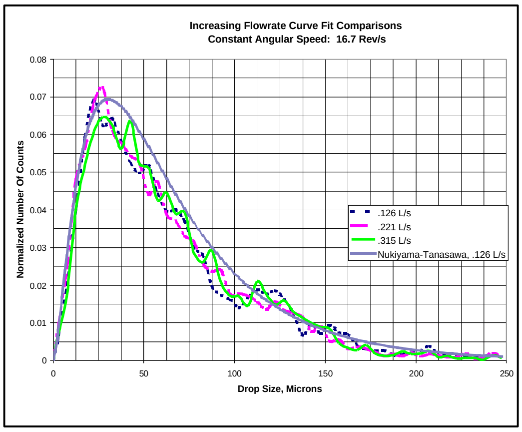

Figure 5b. Drop size distributions for base cases; increasing flow rate.

comparing the D30s and the D30 error ranges for the test condition data [4]. If the D30 for a test condition fell into the range of another, then there was no significant difference between the test conditions. If the D30 for a test condition fell outside of the range of another, then there was a significant difference between the test conditions It was found that:

- As the angular speed increased there was a statistical decrease in D30.
- At 10.1 Rev/s, there was no statistical change in the D30 as the flow rate increased.
- At 16.7 Rev/s, as the flow rate increased from .126 to .221 L/s, there was a statistical decrease in D30.
- At 16.7 Rev/s as the flow rate increased from .221 to .315 L/s, there was not a statistical change in D30.

Regarding the PEO Additive test conditions, it was observed that there was a slight apparent change in the drop size distributions with increasing flow rate, specifically a shift to the left, to lower drop diameters. A statistical test was also performed on the data and it was found that there was a statistical difference between these data sets, with the lower flow rate characterized by a higher D30. This could very well be due to the greater entrainment of tiny drops with a higher density of fluid ligaments that occurs at higher flow rates.

Shown in Figure 6 is the chart of the drop size distribution of the coolant with the PEO relative to the base case at .126 L/s and 16.7 Rev/s. There is a noticeable shift in the drop size distributions to a higher mean diameter with the addition of the PEO relative to that of the base cases. The same behavior was observed at the higher flow rate. This was to be expected due to the formation of larger drops at breakup with the PEO. There was also a change in the shape of the drop size distribution from a lognormal form to a more normal form. A statistical test was performed and it was found that there was a statistical increase in D30 (and D10) due to the addition of the PEO Additive.

Regarding the Smooth Topography testing, it was observed that there is an apparent change in the drop size distributions with increasing flow rate, specifically a slight shift to the right, to higher drop diameters. However, there is also a significant shortening and spreading of the distribution at the lower flow rate, resulting overall in a higher D10 at the lower flow rate. A statistical test was performed on the data that validated this observation. This could very well be due to the same reason as that attributed to the shift in the PEO Additive testing, i.e., a greater entrainment of tiny drops with a higher density of fluid ligaments occurring at higher flow rates. Also, the plateau between 95 to 130 μm observed in the base case distributions and in the PEO Additive distributions was absent in the Smooth

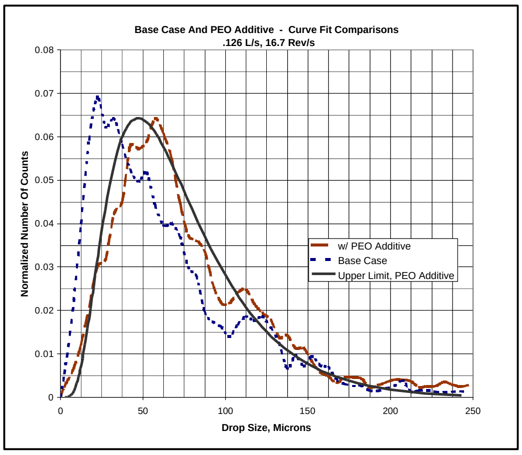

Figure 6. Drop size distributions for base case and PEO Additive testing.

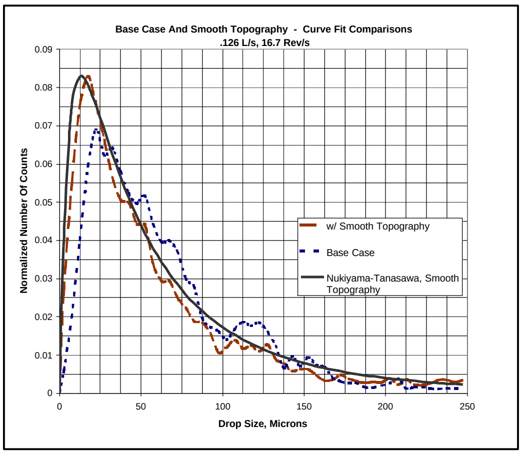

Figure 7. Drop size distributions for base case and Smooth Topography testing.

Topography distributions. Thus it appears that the rough surface topography of the milling cutter peripheral surface is responsible for the observed plateaus in the base cases and the PEO Additive cases. Shown in Figure 7 is the chart of the drop size distribution for the Smooth Topography testing relative to the base case at .126 L/s and 16.7 Rev/s. A statistical test was performed and it was found that there was a statistical difference in the D30 of Smooth Topography testing and the base case testing only at the higher flow rate.

The drop size distributions for all the test conditions were curve fit using the four most well know distributions equations/functions for spray data[5]. These are the Rosin-Rammler Equation, the Nukiyama-Tanasawa Equation, the Log Probability Function, and Upper Limit Function. It was found that the Nukiyama-Tanasawa Equation best fit the base case and Smooth Topography data, while the Upper Limit Function best fit the PEO Additive data. These curve fits are also charted in Figures 5b, 6 and 7.

3.3 Data Rates In The Source Data Region

Regarding the base case testing, the data rates increased by a factor of 3.44 to 4.78 as the angular speed increased, the flow rate held constant. When comparing data for test conditions with a varying flow rate, constant angular speed, the data rates did not change as much, decreasing by a factor of 1.21 to 1.46 as the flow rate increased from .126 to .221 L/s, then stabilizing thereafter. Thus there was a decrease in data rates by a factor of 1.21 to 1.46 as the flow rate increased from .126 to .315 L/s. This same trend was observed with increasing flow rate for the testing involving the PEO Additive and the Smooth Topography where the factors representing the decrease in data rates were 1.35 and 1.27 respectively. This decrease in data rate with increasing flow rate is due to the following 3 reasons: a greater fluid cushioning effect as the MWF jet struck the cutter, resulting in larger drops initially produced at breakup; more low speed collisions of small drops resulting in small drop coalescence; the small drops being entrained with the body of fluid funneled downward from the cutter, i.e., in the white streams of fluid observable in Figure 1.

It is also to be observed by studying Table 1 that the data rates were lower by a factor of 1.26 to 1.36 for the cases involving the PEO Additive testing relative to the base cases, and lower by a factor of 3.01 to 3.45 for the cases involving the Smooth Topography testing. The PEO Additive testing resulted in lower data rates relative to the base cases due to the ligaments and large drops formed upon breakup being able to hold themselves together better. The Smooth Topography testing resulted in lower count rates due to the greater amount of dispersion of the spray relative to the base cases.

3.4 Velocity Vectors In The Source Data Region

A statistical analysis, similar to the ones discussed above, was performed on the velocity vectors of the drops of size 30 μm and less to determine if they were statistically different from one test condition to another. It was found that they were all statistically different, and followed the trends as listed in Table 1.

It can be seen by studying Table 1 that the velocity vector magnitudes decreased for the base cases with increasing coolant flow rate. This was due to the location of PDPA data collection, which was farther from the cutter edge and farther from the spray birth point at the higher flow rate (.315 L/s). The velocity vector angles also decreased with increasing flow rate for the base cases, also due to the data being taken farther out from the cutter edge. The decrease in both the velocity magnitude and angle with increasing flow rate was also due to greater entrainment by the body of fluid funneled downward from the cutter. The velocity vector magnitude and angle of the drops increased with increasing cutter peripheral speed as expected.

For the PEO Additive cases, the velocity vector magnitude apparently increased with increasing flow rate. This was also statistically proven to be true. This was due to the data collection locations of the PEO Additive tests. The data was collected at approximately the same location at both flow rates. The velocities were higher at the higher flow rate due to less shear energy losses of the droplets when surrounded by a greater volume of drops. The velocity vector angle correspondingly decreased with increasing flow rate due to the greater entrainment by the body of fluid drops at higher flow rates. Relative to the base cases, at the low flow rate the velocity vector decreased while at the high flow rate the velocity vector increased. The former is due to the fact that the PEO Additive MWF has a greater molecular weight thus feels the force of gravity more readily, while the latter is due to fact that the data was taken much closer along the trajectory to the birth point. At both flow rates, the lower angle observed is due to the high molecular weight of the PEO Additive MWF relative to the base cases

For the Smooth Topography cases, the velocity vectors increased with increasing flow rate, as can be observed in Table 1. This was also statistically proven to be true. The reason for this increase in velocity vector magnitude with increasing flow rate is the same physics as that for the PEO Additive testing. Valid PDPA data collection locations were the same for both flow rates for the Smooth Topography testing, however there was a much denser body of ligaments entraining the small drops at the higher flow rate. Relative to the base cases, the Smooth Topography testing resulted in smaller velocity vector magnitudes and angles. This was due to a greater dispersion of the spray produced from the Smooth Topography testing. The drops were more affected by shear forces due to a greater surface area of the drops being in contact with still air relative to the base cases. The absence of funneling and flinging of the fluid outward from the cutter of the Smooth Topography spray also resulted in a decrease in spray angle for the Smooth Topography testing relative to the base cases.

Conclusions

PDPA data was taken for eleven different test conditions involving variations on the coolant flow rate, the cutter angular speed, the type of coolant, and the cutter surface topography for wet face milling. Drop size, drop count rate, and particle velocity information was collected and studied. This data will be used to create CFD models of MWF sprays dispersing in manufacturing environments.

Little difference in the drop size distributions occurred due to variations on the coolant flow rate and the cutter angular speed. Utilizing a coolant with a PEO additive resulted in a shift forward in the drop size distribution to higher drop diameters. This was due to the high elongational viscosity of the PEO additive. Utilizing a cutter with a smooth surface topography resulted in a shift backward in the drop size distribution to lower drop diameters. This is attributed to less coalescence of the small drops and to less entrainment of the small drops in fluid streams. The data rates decreased with increasing flow rate and increased with increasing cutter angular speed. The decrease in data rate with increasing flow rate is due to the greater entrainment of the small drops in the fluid sheets flung off the cutter with increasing mass flow rate. The data rates decreased when utilizing the coolant with the PEO and when utilizing the cutter with the smooth surface topography. The data rates decreased when using the PEO due to more large drops formed when the MWF jet impinged upon the spinning cutter, i.e., at the spray birth. The data rates decreased when using the smooth cutter topography due to the greater dispersion of drops encouraged by the smooth topography relative to the serrated milling cutter peripheral. Both the velocity vector magnitudes and angles decreased with increasing flow rate due to increasing entrainment of the small drops with increasing flow rate. Both the velocity vector magnitudes and angles increased with increasing cutter angular speed as expected. The velocity vector magnitude increased when utilizing the coolant with the PEO at a high flow rate but not at a low flow rate due to the data collection location. The velocity vector angle decreased when utilizing the coolant with the PEO due to the high molecular weight of the PEO. Both the velocity vector magnitude and angle decreased when utilizing the cutter with a smooth surface topography due to the absence of funnelling which was experienced with the milling cutter surface.

References

[1] Geier P, Kim H, Xie X, and Lai M C 2002 *ILASS Americas, 15th Annual Conference on Liquid Atomization and Spray Systems* 105-9

[2] http://www.tsi.com/fluid/products/part/part.htm

[3] Gulari E, Manke C W, Yurgelevic S, and Smolinski J 1997 *Metal Working Fluids Symposium II. The Industrial Metalworking Environment: Assessment and Control of Metal Removal Fluids* 291-6

[4] Box E P, Hunter W G, and Hunter J S 1978 *Statistics For Experimenters* (U.S.A.: John Wiley & Sons, Inc.)

[5] Mugele R A, and Evans H D 1951 *Industrial and Engineering Chemistry* **43** 1317-24